

A Novel Approach to Fingerprint Identification Using Gabor Filter-Bank

Ms.Prajakta M. Mudegaonkar¹, Prof.Ramesh P. Adgaonkar²

¹ Student of Master of Engineering in Computer Science, GSM's Marathwada Institute of Technology,
Beed By-Pass Road, Aurangabad, Maharashtra, India.
Email: pmm997@gmail.com

² Department of Computer Science and Engineering, GSM's Marathwada Institute of Technology,
Beed By-Pass Road, Aurangabad, Maharashtra, India.
Email: rp_adgaonkar@rediffmail.com

Abstract "Fingerprint Identification is a widely used Biometric Identification mechanism. Up till now different techniques have been proposed for having satisfactory Fingerprint Identification. The widely used minutiae-based representation did not utilize a significant component of the rich discriminatory information available in the fingerprints. Local ridge structures could not be completely characterized by minutiae. The proposed filter-based algorithm uses a bank of Gabor filters to capture both local and global details in a fingerprint as a compact fixed length Finger Code. The Fingerprint Identification is based on the Euclidean distance between the two corresponding Finger Codes and hence is extremely fast and accurate than the minutiae based one. Accuracy of the system is 98.22%.

Index Terms "Core Point, Euclidean Distance, Fingerprints, Feature Vector, Finger Code, Gabor Filter-bank.

I. INTRODUCTION

Fingerprint-based identification is one of the most important biometric technologies which has drawn a substantial amount of attention recently. Humans have used fingerprints for personal identification for centuries and the validity of fingerprint identification has been well established. Among all the biometrics fingerprint-based identification is one of the most mature and proven technique. Fingerprints are believed to be unique across individuals and across fingers of same individual [1],[2]. These observations have led to the increased use of automatic fingerprint-based identification in both civilian and law-enforcement applications. A fingerprint is the pattern of ridges and valleys on the surface of a fingertip. When fingerprint image is analyzed at global level, the fingerprint pattern exhibits one or more regions where ridge lines assume distinctive shapes. These shapes are characterized by high curvature, terminations, bifurcations, cross-over *etc.* These regions are called singular regions or singularities [5]. These singularities may be classified into three topologies; loop, delta and whorl. At local level, there are other important features known as minutiae can be found in the fingerprint patterns. Minutiae mean small details and this refers to the various ways that the ridges can be discontinuous. A ridge can suddenly come to an end which is called termination or it can divide into two ridges which is called bifurcations as shown in Fig. 1 [5].

Although the fingerprints possess the discriminatory information, designing a reliable automatic fingerprint matching algorithm is very challenging. As fingerprint sensors are becoming smaller and cheaper, automatic identification based on fingerprints is becoming an attractive alternative/complement to the traditional methods of identification. The critical factor in the widespread use of fingerprints is in satisfying the performance (*e.g.*, matching speed and accuracy) requirements of the emerging civilian identification applications [2]. Some of these applications (*e.g.*, fingerprint-based smartcards) will also benefit from a compact representation of a fingerprint.

II. FINGERPRINT IDENTIFICATION

Fingerprint matching techniques can be broadly classified as minutiae based and correlation based [5]. Minutiae based technique first located the minutiae points in a given fingerprint image and matched their relative placements in a stored template. The performance of this technique relied on the accurate detection of minutiae points and the use of sophisticated matching techniques to compare two minutiae fields which undergo non-rigid transformations. Correlation based techniques compared the global pattern of ridges and valleys to see if the ridges in the two fingerprints align. The global approach to fingerprint representation was typically used for indexing and did not offer reliable fingerprint discrimination.



Fig.1 Ridge ending, core point and ridge bifurcation

The ridge structure in a fingerprint can be viewed as an oriented texture patterns having a dominant spatial frequency and orientation in a local neighborhood. The frequency is due to inter ridge-spacing present in a fingerprint and the orientation is due to the flow pattern exhibited by ridges. By capturing the frequency and orientation of ridges in local regions in the fingerprint, a distinct representation of the fingerprint is possible. In this paper I mainly focused on Gabor Filter-bank based Fingerprint Identification..Since Gabor Filters are characterized by spatial frequencies and orientation capabilities, they are best suited for fingerprint identification [3]. Single Gabor Filter function was not sufficient for capturing whole global and local fingerprint information therefore bank of Gabor filters was prepared with 8 Gabor Filters. Detailed filter-bank based feature extraction procedure is discussed in upcoming sections.

III. GABOR FILTER-BANK BASED FEATURE EXTRACTION

In the proposed system initially core point in fingerprint image was detected [2],[5]. The core point corresponds to center of loop type singularity. Some fingerprints did not contain loop or whorl singularities, therefore it was difficult to define core. In that kind of images, core is normally associated with the maximum ridge line curvature. Detecting a core point was not a trivial task. For finding core point, initially orientation field was estimated. [7],[8],[9]. For that one algorithm is discussed here. Fig. 2 shows an optimal core point in an fingerprint image, as in [5].After getting a core point, circular region around the core point was tessellated into 80 sectors. The pixel intensities in each sector were normalized to a constant mean and variance. The circular region was filtered using a bank of eight Gabor filters to produce a set of eight filtered images. The average absolute deviation with in a sector quantifies the underlying ridge structure and was used as a feature. A feature vector (640 bytes in length) was collection of all the features, computed from all the 80 sectors, in every filtered image. The feature vector captured the local information and the ordered enumeration of the tessellation captured the invariant global relationships among the local patterns. The matching stage computed the Euclidean distance between the two corresponding feature vectors. It is desirable to obtain representations for



Fig. 2 Optimal Core Point Location

fingerprints which are translation and rotation invariant. In the proposed scheme, translation was taken care of by core point during the feature extraction stage and the image rotation was handled by a cyclic rotation of the feature values in the feature vector. The features were cyclically rotated to generate feature vectors corresponding to different orientations to perform the matching.

A. Core Point Detection

For having satisfactory Fingerprint Identification, finding exact reference point or core point was an important task. Since core point was nothing but a high curvature region in the fingerprint, it's totally dependent on the orientation of ridges. Therefore orientation field of the fingerprint was estimated. The typical orientation field of a fingerprint is shown in Fig. 3 as in [8].Steps for orientation field estimation are discussed below. Let $\hat{\theta}$ be defined as the orientation field of a finger print image. $\hat{\theta}(i,j)$ represents the local ridge orientation at pixel (i,j) . Local ridge orientation, however, was usually specified for a block rather than that of every pixel. Thus, an image was divided in to a set of non-overlapping blocks of size $w \times w$. Each block held a single orientation. In connection with the work outlined in this paper, the smoothed orientation field based on least mean square algorithm is summarized as follows as in [2],[8] :

1. The input image I was divided into non-overlapping blocks with size $w \times w$.
2. Gradients $\hat{a}_x(i,j)$ and $\hat{a}_y(i,j)$ were calculated, at each pixel (i,j) which was the center of the block.
3. Local orientation was estimated using the following equations :

The gradient operator can be chosen according to the computational complexity. Generally sobel operator is used.

$$V_x(i,j) = \sum_{u=i-\frac{w}{2}}^{i+\frac{w}{2}} \sum_{v=j-\frac{w}{2}}^{j+\frac{w}{2}} 2\partial_x(u,v) \partial_y(u,v) \quad (1)$$

$$V_y(i,j) = \sum_{u=i-\frac{w}{2}}^{i+\frac{w}{2}} \sum_{v=j-\frac{w}{2}}^{j+\frac{w}{2}} 2\partial_x^2(u,v) \partial_y^2(u,v) \quad (2)$$

Subsequently,



Fig. 3 Fingerprint Orientation Map (a) Orientation Field mapped over Fingerprint (b) Orientation Field Map

$$\theta(i,j) = \frac{1}{2} \tan^{-1} \left[\frac{V_y(i,j)}{V_x(i,j)} \right] \quad (3)$$

local ridge orientation at the block with the centered at pixel (i,j) .

4. The discontinuity of ridge and valley due to noise could be softened by applying a low pass filter. However, to apply a low pass filter the orientation image must be converted to a continuous vector field. The continuous vector field, which its x and y components are defined as Φ_x and Φ_y respectively.

$$\Phi_x(i, j) = \cos(2\theta(i, j)) \quad (4)$$

$$\Phi_y(i, j) = \sin(2\theta(i, j)) \quad (5)$$

With the resulted vector field, the two dimensional low-pass filter G with unit integral was applied. The specified size of the filter was $w_\Phi \times w_\Phi$, as a result,

$$\Phi'_x(i, j) = \sum_{u=-w_\Phi/2}^{w_\Phi/2} \sum_{v=-w_\Phi/2}^{w_\Phi/2} G(u, v) \cdot \Phi_x(i - uw, j - vw) \quad (6)$$

$$\Phi'_y(i, j) = \sum_{u=-w_\Phi/2}^{w_\Phi/2} \sum_{v=-w_\Phi/2}^{w_\Phi/2} G(u, v) \cdot \Phi_y(i - uw, j - vw) \quad (7)$$

5. The smoothed orientation field local ridge orientation at (i, j) was then computed as follows:

$$O'(i, j) = \frac{1}{2} \tan^{-1} \left[\frac{\Phi'_y(i, j)}{\Phi'_x(i, j)} \right] \quad (8)$$

Now after finding out the smoothed orientation field, core point was found out. For locating this reference point I had implemented integration of sine components method. Therefore further steps according to this method are given below:

6. Value \hat{a} was computed, an image containing only the sin component of O' .

$$\varepsilon(i, j) = \sin(O'(i, j)) \quad (9)$$

7. A label image A was used to indicate the reference point. For each pixel (i, j) in \hat{a} , pixel intensities (sine component of the orientation field) were integrated in regions R_I and R_{II} as shown in Fig. 4 and the corresponding pixels were assigned in A , the value of their difference was calculated as:

$$A(i, j) = \sum_{R_I} \sin(O(i, j)) - \sum_{R_{II}} \sin(O(i, j)) \quad (10)$$

The regions R_I and R_{II} (see Fig. 4) were determined empirically by applying the reference point location algorithm over a large database. The geometry of these regions was designed to capture the maximum curvature in concave ridges. 8. Maximum value in A was found out and its co-ordinates were assigned to the core point [2]. By repeating the steps fixed number of times for different window sizes, accurate core point was calculated. However, this method was not able to find out correct core point in an arch type of singularities. According to some authors it's beneficial to combine two-three methods for detecting accurate core point as in [9].

B. Tessellation of Region of Interest

After finding out the core point, the circular region around this core point was tessellated into sectors as in [2]. I used 5

concentric bands around core point. Each band is 20 pixels wide and segmented into sixteen two sectors. Thus there were total $16 \times 5 = 80$ sectors and the region of interest was a circle of radius 100 pixels, centered at the core point. The tessellated region of interest is shown in Fig. 5.

IV. FILTERING

Before filtering the fingerprint image, the region of interest was normalized in each sector separately to a constant mean and variance. Normalization was performed to remove the effects of sensor noise and gray level deformation due to finger pressure differences as given in [3],[5]. $I(x, y)$ denoted the gray value at pixel (x, y) , M_i and V_i , the estimated mean and variance of sector S_i , respectively, and $N_i(x, y)$, the normalized gray-level value at pixel (x, y) . For all the pixels in sector S_i , the normalized image was defined as:

$$N_i(x, y) = \begin{cases} M_0 + \sqrt{\frac{V_0 \times (I(x, y) - M_i)^2}{V_i}}, & \text{if } I(x, y) > M_i \\ M_0 - \sqrt{\frac{V_0 \times (I(x, y) - M_i)^2}{V_i}}, & \text{otherwise} \end{cases} \quad (11)$$

Where M_0 and V_0 were the desired mean and variance values, respectively. Values of them were already set according to experimental conditions. Normalization was a pixel-wise operation which did not change the clarity of the ridge and valley structures. If normalization was performed on the entire image, then it could not compensate for the intensity variations in different parts of the image due to the elastic nature of the finger. Separate normalization of each individual sector alleviated this problem. Fig. 6 shows normalized image. Gabor filters optimally capture both local orientation and frequency information from a fingerprint image. By

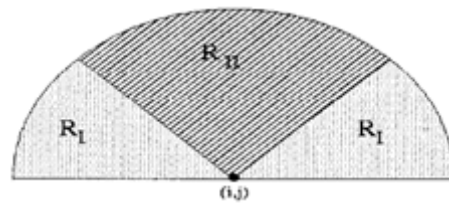


Fig. 4 Regions for integrating \hat{a} pixel intensities for $A(i, j)$

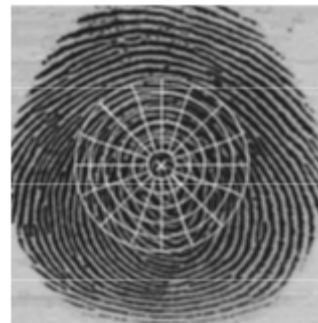


Fig. 5 Core point (\times), Region of interest and 80 sectors Superimposed on a fingerprint

tuning a Gabor filter to specific frequency and direction, the local frequency and orientation information can be obtained..Thus, they are suited for extracting texture information from images. An even symmetric Gabor filter had the following general form in the spatial domain as in [4],[6]:

$$G(x, y; f, \theta) = \exp \left\{ -\frac{1}{2} \left[\frac{x'^2}{\delta_{x'}^2} + \frac{y'^2}{\delta_{y'}^2} \right] \right\} \cos(2\pi f x') \quad (12)$$

$$x' = x \sin \theta + y \cos \theta \quad (13)$$

$$y' = x \cos \theta - y \sin \theta \quad (14)$$

where f was the frequency of the sinusoidal plane wave along the direction θ from the x-axis, $\delta_{x'}$ and $\delta_{y'}$ were the space constants of the Gaussian envelope along x' and y' axes, respectively. It's beneficial to set the filter frequency f to the average ridge frequency ($1/K$), where K was the average inter-ridge distance. I used eight different values for θ (0, 22.5, 45, 67.5, 90, 112.5, 135, and 157.5) with respect to the x-axis. The normalized region of interest (see Fig.6) in a fingerprint was convolved with a 0°-oriented filter accentuates those ridges which are parallel to the x-axis and smoothes the ridges in the other directions. Filters tuned to other directions work in a similar way. These eight directional-sensitive filters captured most of the global ridge directionality information as well as the local ridge characteristics present in a fingerprint. Fig. 7 shows filtering in different directions, as in [2], [4].

V. FEATURE VECTOR

Let $F_{i\theta}(x, y)$ be the θ -direction filtered image for sector S_i . Now, $\forall i \in \{0, 1, \dots, 79\}$ and $\theta \in \{0^\circ, \dots, 157.5^\circ\}$, the feature value, $V_{i\theta}$, was the average absolute deviation from the mean defined as :

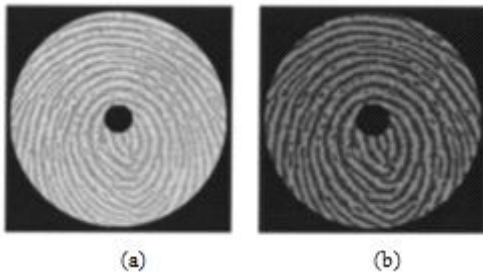


Fig. 6 Fingerprint Images: (a) Area of Interest (b) Normalized Image

$$V_{i\theta} = \frac{1}{n_i} (\sum_{n_i} |F_{i\theta}(x, y) - P_{i\theta}|) \quad (15)$$

where n_i was the number of pixels in S_i and $P_{i\theta}$ was the mean of pixel values of $F_{i\theta}(x, y)$ in sector S_i . The average absolute deviation of each sector in each of the eight filtered images defined the components of our feature vector. In this way a 640-dimensional feature vectors were formed. Fig. 8 shows examples of 640-dimensional feature vectors for fingerprints.

VI. MATCHING

Fingerprint matching was based on finding the Euclidean distance between the corresponding Finger Codes. The translation invariance in the Finger Code was established by the reference point. Approximate rotation invariance was achieved by cyclically rotating the features in the Finger Code itself. For each fingerprint 5 templates were stored in the database. Test fingerprint template was matched with all the 5 templates of each fingerprint and scores were noted [2]. The minimum score corresponded to the best alignment of the two fingerprints being matched. If the Euclidean distance between two feature vectors was less than a threshold, then the decision that “the two images come from the same finger” was made, otherwise a decision that “the two images come from different fingers” was made.

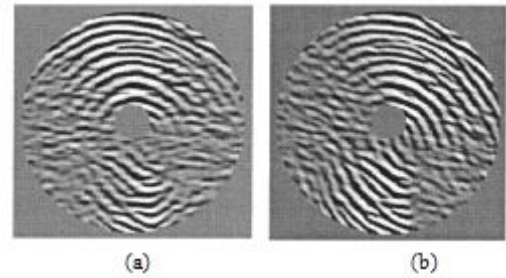


Fig.7 Filtered Images (a) 0° (b) 22.5° similarly up to 157.5°. While four directions are sufficient for classification; eight directions are needed for fingerprint identification.

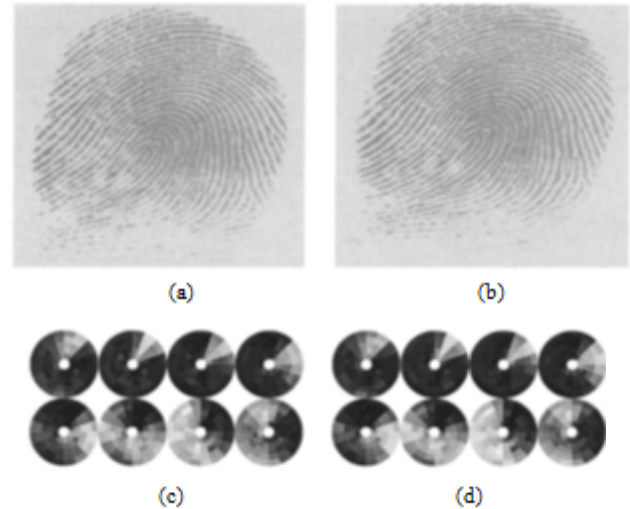


Fig.8 Examples of 640-dimensional feature vectors: (a) First impression of finger 1, (b) second impression of finger 1, (c) Finger Code of (a), (d) Finger Code of (b)

Since the template generation for storage in the database was an off-line process, the verification time still dependent on the time taken to generate a single template.

VI. EXPERIMENTAL RESULTS

For performing the whole procedure I used FVC 2000 database. In this database there were eight fingerprint scans per person and total there are 80 scans of 10 persons. When the Gabor Filter-Based Fingerprint Identification was applied on this database I got overall 98.22% accuracy. The accuracy

was measured in terms FRR (False Rejection Rate) and FAR (False Acceptance Rate). That's why this method was found more reliable and extremely faster than the minutiae-based fingerprint matching.

CONCLUSIONS

Fingerprint Identification is one of the well known and reliable Biometrics Authentication Techniques. Here I discussed a Gabor filter-bank based technique for fingerprint Identification. Gabor filters are characterized by frequency and orientation a component that's why they are perfectly suitable for fingerprint Identification. The primary advantage of this approach was its computationally attractive matching/indexing capability. For instance, if the normalized (for orientation and size) Finger Codes of all the enrolled fingerprints were stored as templates, the identification effectively involves a "bit" comparison. As a result, the identification time would be relatively insensitive to the database size. The accuracy achieved in terms of FRR and FAR was 98.22%. Therefore the whole discussion in this paper concluded that this system performs better than the minutiae-based system.

REFERENCES

- [1] S.Mahadik, K.Narayanan, D.V.Bhoir, D .Shah," Access control system using fingerprint recognition", *International Conference on Advances in Computing, Communication and Control*, vol.3, 2009.
- [2] A.K.Jain, S.Prabhakar, L.Hong, S.Pankanti, " Filter bank – based fingerprint matching", *IEEE Transactions on Image Processing*, vol.9, no..5, pp.846- 859, May 2000.
- [3] C.J. Lee, S .D.Wang," A Gabor filter-based approach to fingerprint recognition", unpublished.
- [4] M.Huppmann," Fingerprint recognition by matching of gabor filter-based patterns", unpublished.
- [5] M.Umer Munir and Dr. M.Y. Javed," Fingerprint matching using gabor filters", unpublished.
- [6] J.R.Movellan,"Tutorial on gabor filters", unpublished.
- [7] M. Liu, X. Jiang , A. C . Kot," Fingerprint reference–point detection", *EURASIP Journal on Applied Signal Processing*, vol.4, pp. 498-509, 2005.
- [8] H. B. Kekre,V.A. Bharadi,"Fingerprint core point detection algorithms using orientation field based multiple features",*International Journal of Computer Applications* vol.1, pp. 97- 103.
- [9] A. Julasayvake, S. Choomchuay," Combined technique for fingerprint core point detection",unpublished.